

Dynamic Event-Triggered Control of Discrete-Time Nonlinear Systems based on Difference-Algebraic Representations^{*}

Vitoriano Medeiros Casas^{*}, Gabriela Lígia Reis^{**},
Pedro Henrique Silva Coutinho^{***}, Iury Bessa^{****},
Rodrigo Farias Araújo[†]

^{*} Graduate Program in Electrical Engineering, Federal University of Amazonas, Av. Gen. Rodrigo Octávio, 6200, Manaus, AM, Brazil (e-mail: vitoriano.casas@ufam.edu.br)

^{**} Department of Technological Education, Federal Institute of Southeast Minas Gerais, R. Bernardo Mascarenhas, 1283, Juiz de Fora, MG, 36080-001, Brazil (e-mail: gabriela.reis@ifsudestemg.edu.br)

^{***} Department of Electronics and Telecommunication Engineering, State University of Rio de Janeiro, Av. São Francisco Xavier, 524, Rio de Janeiro, RJ, 20550-900, Brazil (e-mail: phcoutinho@eng.uerj.br)

^{****} Faculty of Electrical and Computer Engineering, Federal University of Amazonas, Av. Gen. Rodrigo Octávio, 6200, Manaus, AM, Brazil (e-mail: iurybessa@ufam.edu.br)

[†] Department of Control and Automation Engineering, Amazonas State University, Av. Darcy Vargas, 1200, Parque 10 de Novembro, Manaus, AM, 69050-020, Brazil (e-mail: rfaraujo@uea.edu.br)

Abstract: This paper addresses the dynamic event-triggered control for a class of discrete-time nonlinear systems described by a difference-algebraic representation (DAR), using a gain-scheduled controller. An outstanding aspect of the proposed method is the incorporation of information about the system's nonlinearities into the control law and the trigger function. The proposed event-triggered mechanism also incorporates information on the asynchronous terms induced by the event-based sampling. All these ingredients enable the derivation of a less conservative co-design condition for the simultaneous design of the gain-scheduled control law and the dynamic triggering mechanism to ensure the asymptotic stability of the closed-loop system. An estimate of the region of attraction of the origin of the closed-loop system is obtained to guarantee the closed-loop system's operation within the domain of validity of the DAR. Then, an optimization problem is formulated to reduce the number of events and enlarge the estimated region of attraction. Finally, the effectiveness of the proposed condition is illustrated by a numerical example.

Keywords: Event-based control; Convex optimization; Difference-Algebraic Representation; Lyapunov methods; Control over networks.

1. INTRODUCTION

Event-triggered control (ETC) is a relevant strategy for providing efficient implementations of networked control systems (NCS). Unlike traditional time-triggered approaches, which perform periodic or aperiodic transmissions regardless of the system's state, ETC performs control updates only when certain conditions related to the dynamic behavior of the system are violated Abdelrahim et al. (2018).

The main motivation behind ETC lies in reducing the rate of transmitted data over the communication network,

^{*} This work was supported by the Brazilian agencies CNPq (Grant numbers: 407885/2023-4, 307758/2025-7; 308791/2025-8), CAPES, and FAPEAM.

relieving congestion, and allowing the control scheme to operate effectively even in the presence of delays and packet losses in shared environments. The key component of ETC systems is the Event-Triggering Mechanism (ETM), which is responsible for monitoring the system and determines when a new data transmission is required. This mechanism evaluates the plant measurements and determines transmission times based on previously defined triggering conditions Abdelrahim et al. (2018).

The ETM can be classified as static, adaptive, or dynamic. Dynamic ETC incorporates an internal variable whose growth rate depends on the system's state, helping to suppress unnecessary transmissions more efficiently Girard (2015). For discrete-time systems, an increasing number of works have addressed event-triggered control Hu et al.

(2016); Xiao et al. (2021). Dynamic mechanisms have been widely studied for discrete-time systems, particularly in linear settings, where they are known to extend inter-event intervals while preserving stability Girard (2015); Abdelrahim et al. (2018). Xu et al. (2023) proposes an observer-based dynamic event-triggered control strategy for discrete-time linear multi-agent systems. In Li et al. (2021), adaptive control problems for unknown second-order nonlinear multi-agent systems are investigated. In Zuo et al. (2019); Coutinho and Palhares (2021, 2022), the co-design conditions for dynamic ETC of nonlinear systems are presented based on a gain-scheduling approach to quasi-LPV models. Despite these contributions to discrete-time systems, most studies focus on linear dynamics, and there remains a gap in the study of nonlinear systems.

Nonlinear control strategies can often improve closed-loop system performance. One common approach to handling nonlinear systems involves using polytopic inclusions, where the nonlinear dynamics are represented by a convex combination of linear vertex systems, with weighting functions that depend on parameters or scheduling variables evolving within a predefined convex region. This representation allows the use of linear matrix inequalities (LMIs) constraints and convex optimization techniques to design controllers that guarantee stability within the polytopic region.

Among the various representations of nonlinear systems by means of polytopic inclusions, the differential-algebraic representation has attracted attention due to its capability to model a wide range of real-world nonlinear systems and phenomena Oliveira et al. (2013a). While standard polytopic models approximate nonlinear dynamics through convex combinations of linear systems, the differential-algebraic representation is capable of providing equivalent representations of rational systems through a set of algebraic and differential equations Reis et al. (2021). In the discrete-time context, difference-algebraic representations (DAR) have been proposed by Coutinho et al. (2009). These representations allow the use of a polytopic formulation for nonlinear systems and the development of LMI-based conditions derived from the application of Lyapunov theory.

Many works have employed DAR for controlling nonlinear systems. DAR-based formulations have been applied to estimate the region of attraction of nonlinear systems with saturating actuators Coutinho and Gomes da Silva Jr. (2010) and to address robust stability under uncertainties Rohr et al. (2009). In the context of discrete-time systems, Oliveira et al. (2013b) has proposed a condition for the stability of nonlinear systems subject to disturbances and actuator saturation. DAR has also been applied to the region of attraction (RoA) estimation Oliveira et al. (2013b, 2012); Azizi et al. (2018). Few works have addressed the ETC of nonlinear systems using DAR. In Moreira et al. (2017), a method for static ETC design of continuous-time rational systems is proposed, employing an emulation-based approach. In a different approach, Moreira et al. (2020) develops a co-design condition. More recently, the dynamic ETC has been studied in Reis et al. (2025). However, it still lacks developments for ETC design based on DAR for discrete-time nonlinear systems, particularly

concerning dynamic ETC, which is the problem pursued in this paper.

A central issue in applying ETC to nonlinear controllers, especially gain-scheduling schemes, is asynchronism, which induces a mismatch between the actual current state of the system and the last state received by the controller. To incorporate the effects of asynchronism in the polytopic representation, a cancellation-based approach is adopted in Coutinho and Palhares (2022); Coutinho et al. (2022); Reis et al. (2025); Pessim et al. (2023); Coutinho et al. (2025), where an additional term is introduced in the triggering function to mitigate asynchronism. In this context, this paper proposes the following: (I) A dynamic ETC for discrete-time nonlinear rational systems in DAR form that includes an additional term to deal with the asynchronism; (II) Co-design conditions for a dynamic ETM and a nonlinear controller. The controller is designed to utilize nonlinearity information and is capable of asymptotically stabilizing the systems under polytopic inclusions; (III) An optimization problem focused on minimizing the number of events while simultaneously expanding the region of attraction.

The remainder of this paper is structured as follows. The problem formulation is stated in Section 2. Section 3 develops the co-design methodology for the proposed ETC strategy at the same time that the estimate of the region of attraction is maximized. Section 4 presents numerical experiments that illustrate the effectiveness of the proposed method and validate the co-design conditions. Concluding remarks are provided in Section 5.

Notation. \mathbb{N} is the set of positive integers, $\mathbb{N}_{\leq p}$ the set of positive integers less than or equal to $p \in \mathbb{N}$, \mathbb{N}_0 is the set of nonnegative integers, $\mathbb{B} = \{0, 1\}$ is the Boolean domain, \mathbb{R}^n is the n -dimensional Euclidean space, $\mathbb{R}^{n \times m}$ is the set of $n \times m$ real matrices, and $\mathbb{R}_{\geq 0}$ ($\mathbb{R}_{> 0}$) is the set of nonnegative (positive) real numbers. For a symmetric block matrix, the symbol $*$ denotes the term deduced by symmetry, $\text{diag}(\cdot)$ stands for a block-diagonal matrix, and $\text{He}(M)$ represents $M + M^\top$. $\lambda_{\min}(M)$ ($\lambda_{\max}(M)$) denotes the minimum (maximum) eigenvalue of matrix M . I and 0 denote the identity and null matrices of appropriate dimensions, respectively. Given a multi-index $\mathbf{i} = (i_1, \dots, i_p) \in \mathbb{B}^p$, where $\mathbb{B}^p = \{\mathbf{i} : i_j \in \mathbb{B}, j \in \mathbb{N}_{\leq p}\}$, it is defined $\mathbb{B}^{p^\top} = \{\mathbf{i} : i_j \leq i_{j+1}, i_j \in \mathbb{B}, j \in \mathbb{N}_{p-1}\}$ and $\mathcal{P}(\mathbf{i})$ is the set of permutations of the entries of \mathbf{i} .

2. PROBLEM FORMULATION

Next, we see a few subsections. Consider the diagram of the NCS with ETM shown in Fig. 1. In the considered setup, the plant is a nonlinear system whose state x_k , indexed by $k \in \mathbb{N}_0$, is transmitted to the controller via a general-purpose communication network with transmission instants determined by the triggering policy of the ETM. The ETM generates a sequence of transmission instants $\{k_j\}_{j=0}^\infty$, where k_j is the j -th transmission instant. Then, the state information available to the controller, \hat{x}_k , is held constant, through a zero-order hold (ZOH) mechanism, until the next transmission instant.

Consider that the plant is described by a discrete-time nonlinear dynamical system as follows:

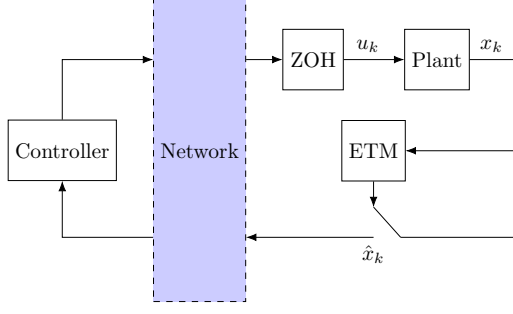


Fig. 1. Networked control system with ETC scheme.

$$x_{k+1} = f(x_k) + g(x_k)u_k \quad (1)$$

where $x_k \in \mathcal{D}_x \subseteq \mathbb{R}^n$ is the state vector of the system and $u_k \in \mathbb{R}^m$ is the control input. The functions $f: \mathbb{R}^n \rightarrow \mathbb{R}^n$, with $f(0) = 0$, and $g: \mathbb{R}^n \rightarrow \mathbb{R}^{n \times m}$, are assumed rational and well-defined on \mathcal{D}_x . Then, the system (1) can be reformulated as a DAR described by Reis et al. (2021); Coutinho and Gomes da Silva Jr. (2010):

$$\begin{aligned} x_{k+1} &= A_1(x_k)x_k + A_2(x_k)\pi_k + A_3(x_k)u_k, \\ 0 &= \Omega_1(x_k)x_k + \Omega_2(x_k)\pi_k + \Omega_3(x_k)u_k, \end{aligned} \quad (2)$$

where $\pi_k \in \mathbb{R}^p$ is the vector of nonlinearities. The matrix-valued functions $A_1(x) \in \mathbb{R}^{n \times n}$, $A_2(x) \in \mathbb{R}^{n \times p}$, $A_3(x) \in \mathbb{R}^{n \times m}$, $\Omega_1(x_k) \in \mathbb{R}^{p \times n}$, $\Omega_2(x) \in \mathbb{R}^{p \times p}$ and $\Omega_3(x) \in \mathbb{R}^{p \times m}$ are affine functions in x and the matrix $\Omega_2(x)$ is square and invertible, for all $x \in \mathcal{D}_x$. The domain of validity of the DAR is given by the following compact polyhedral set:

$$\mathcal{D}_x = \left\{ x_k \in \mathbb{R}^n : b_j^\top x_k \leq 1, j \in \mathbb{N}_{\leq h} \right\} \quad (3)$$

where $b_j \in \mathbb{R}^n$, $j \in \mathbb{N}_{\leq h}$, define the hyperplanes.

Consider the vector π_k written as the solution of the algebraic equation in (2):

$$\pi_k = -\Omega_2^{-1}(x_k) [\Omega_1(x_k)x_k + \Omega_3(x_k)u_k]. \quad (4)$$

The equivalence between the nonlinear system (1) and its DAR (2) can be verified by substituting (4) in the dynamical equation of (2), which results in (1).

Provided that the matrix-valued functions of (2) are affine in x and \mathcal{D}_x is a compact set, each state-dependent element can be bounded by $z_j^0 \leq z_j(x) \leq z_j^1$, for all $j \in \mathbb{N}_{\leq r}$, where r denotes the number of scheduling variables, $z_j(x): \mathcal{D}_x \rightarrow \mathbb{R}$ denotes the j -th scheduling variable, and z_j^0, z_j^1 are its lower and upper bounds, respectively. Then, the DAR system (2) can be equivalently represented as the following polytopic model:

$$\begin{aligned} x_{k+1} &= \sum_{\mathbf{i} \in \mathbb{B}^r} \alpha_{\mathbf{i}}(x_k) (A_{1\mathbf{i}}x_k + A_{2\mathbf{i}}\pi_k + A_{3\mathbf{i}}u_k) \\ 0 &= \sum_{\mathbf{i} \in \mathbb{B}^r} \alpha_{\mathbf{i}}(x_k) (\Omega_{1\mathbf{i}}x_k + \Omega_{2\mathbf{i}}\pi_k + \Omega_{3\mathbf{i}}u_k), \end{aligned} \quad (5)$$

where $\alpha_{\mathbf{i}}(x)$ is given by

$$\alpha_{\mathbf{i}}(x_k) = \prod_{j=1}^r w_{i_j}^j(x_k), \quad (6)$$

where $\mathbf{i} = (i_1, \dots, i_r) \in \mathbb{B}^r$ is an r -dimensional multi-index, and the weight functions are given by

$$w_j^0(x_k) = \frac{z_j^1 - z_j(x_k)}{z_j^1 - z_j^0}, \quad w_j^1(x_k) = 1 - w_j^0(x_k). \quad (7)$$

Thus, the parameters satisfy the convex sum property

$$\sum_{\mathbf{i} \in \mathbb{B}^r} \alpha_{\mathbf{i}}(x) = 1, \text{ and } \alpha_{\mathbf{i}}(x) \geq 0, \quad \forall \mathbf{i} \in \mathbb{B}^r, \forall x \in \mathcal{D}_x. \quad (8)$$

In this work, we employ the following event-triggered gain-scheduled nonlinear control law:

$$u_k = K(\hat{x}_k)\hat{x}_k + L(\hat{x}_k)\hat{\pi}_k, \quad (9)$$

where the state-dependent gains are parameterized as

$$K(\hat{x}) = \sum_{\mathbf{j} \in \mathbb{B}^r} \alpha_{\mathbf{j}}(\hat{x})K_{\mathbf{j}}, \text{ and } L(\hat{x}) = \sum_{\mathbf{j} \in \mathbb{B}^r} \alpha_{\mathbf{j}}(\hat{x})L_{\mathbf{j}}, \quad (10)$$

with $L_{\mathbf{j}} \in \mathbb{R}^{m \times p}$, $K_{\mathbf{j}} \in \mathbb{R}^{m \times n}$, for all $\mathbf{j} \in \mathbb{B}^r$, being the gains to be designed. Moreover, due to the ZOH mechanism, the information on the state \hat{x}_k and the vector of nonlinearities $\hat{\pi}_k$ available to the controller are

$$\hat{x}_k = x_{k_j}, \quad \hat{\pi}_k = \pi_{k_j}, \quad \forall k \in \mathcal{I}_j, \quad (11)$$

where $\mathcal{I}_j := \{k_j, \dots, k_{j+1} - 1\}$ denotes the discrete-time indices between two consecutive transmission instants k_j and k_{j+1} . Then, the transmission errors induced by the event-based sampling are

$$\begin{cases} e_k = \hat{x}_k - x_k, \quad \forall k \in \mathcal{I}_j, \\ \delta_k = \hat{\pi}_k - \pi_k, \quad \forall k \in \mathcal{I}_j. \end{cases} \quad (12)$$

Consider the augmented vector $\zeta = [x^\top \ \pi^\top \ e^\top \ \delta^\top]^\top$. By substituting the control law (9) into the DAR (2), and using the transmission errors (12), the following closed-loop system can be obtained¹:

$$\begin{aligned} x_{k+1} &= x_+ = \varphi_1(\zeta) + \xi_1(\zeta), \\ 0 &= \varphi_2(\zeta) + \xi_2(\zeta), \end{aligned} \quad (13)$$

where

$$\begin{aligned} \varphi_1(\zeta) &= (A_1(x) + A_3(x)K(x))x + A_3(x)K(x)e \\ &\quad + (A_2(x) + A_3(x)L(x))\pi + A_3(x)L(x)\delta, \\ \varphi_2(\zeta) &= (\Omega_1(x) + \Omega_3(x)K(x))x + \Omega_3(x)K(x)e \\ &\quad + (\Omega_2(x) + \Omega_3(x)L(x))\pi + \Omega_3(x)L(x)\delta, \\ \xi_1(\zeta) &= A_3(x)\{(K(x+e) - K(x))(x+e) \\ &\quad + (L(x+e) - L(x))(\delta + \pi)\}, \\ \xi_2(\zeta) &= \Omega_3(x)\{(K(x+e) - K(x))(x+e) \\ &\quad + (L(x+e) - L(x))(\delta + \pi)\}. \end{aligned}$$

Remark 1. Different from the polytopic model of the system (5), whose state-dependent parameters depend on the plant state x_k , the state-dependent gains of the gain-scheduled nonlinear controller (9) depend on the sampled state \hat{x}_k . This leads to the so-called asynchronous phenomenon Coutinho et al. (2025); Coutinho and Palhares (2021, 2022); Reis et al. (2025). The terms induced by the asynchronous phenomenon in the closed-loop dynamics are $\xi_1(\zeta)$ and $\xi_2(\zeta)$. Thus, it is clear that this phenomenon induces an additional internal perturbation to the closed-loop system. If this phenomenon is not properly handled, the gain-scheduling structure of the controller (9) degenerates to a linear control structure, that is, $L_{\mathbf{j}} \approx L$, $K_{\mathbf{j}} \approx K$, $\forall \mathbf{j} \in \mathbb{B}^r$. The solution to deal with this issue will be discussed in the next section.

Based on the previous discussion, this work aims to address the co-design problem of determining a gain-scheduled nonlinear control law (10) operating under a

¹ Hereafter, the discrete-time index is omitted for brevity unless explicitly required.

dynamic ETM for ensuring that the origin of the closed-loop system (13) is asymptotically stable. Moreover, the proposed approach aims to reduce the number of transmissions generated by the ETM and estimate the region of attraction of the origin of (13) within the domain of validity \mathcal{D}_x of the DAR model given in (3).

3. MAIN RESULTS

The main contributions are presented in this section. First, the dynamic ETC scheme and an appropriate trigger function are proposed to compensate for the asynchronous phenomenon between the plant and the controller. Then, a co-design condition is presented to obtain the controller and the ETM parameters. Moreover, the region of attraction of the origin of the closed-loop system is estimated. Finally, an optimization problem is formulated to reduce the number of transmissions and enlarge the estimated region of attraction.

3.1 Dynamic ETM

To reduce the number of transmissions and the usage of communication resources, the transmission instants are determined by the following dynamic ETM:

$$k_{j+1} = \min\{k \in \mathbb{N} : k > k_j \wedge \eta_k + \theta\Gamma(\zeta_k) < 0\}, \quad (14)$$

for all $j \in \mathbb{N}$, where $k_0 = 0$, $\theta \in \mathbb{R}_{>0}$ is a given parameter, and $\eta_k \in \mathbb{R}_{\geq 0}$ is the internal dynamics of the ETM, which evolves according to

$$\eta_{k+1} = (1 - \lambda)\eta_k + \Gamma(\zeta_k), \quad \forall k \in \mathcal{I}_j, \quad (15)$$

where $\lambda \in \mathbb{R}_{>0}$ is a parameter related to the decay rate of η_k . Note that, by construction, the Zeno phenomenon is avoided, since the minimum interval between events is given by a sampling period.

The dynamic ETM (14)–(15) has a trigger function described by

$$\Gamma(\zeta) = x^\top Q_x x + \pi^\top Q_\pi \pi - e^\top Q_e e - \delta^\top Q_\delta \delta - \xi(\zeta), \quad (16)$$

where

$$\xi(\zeta) = 2\varphi_1^\top P \xi_1 + \xi_1^\top P \xi_1 + 2\pi^\top Z \xi_2, \quad (17)$$

The term $\xi(\zeta)$ is to be designed to handle the asynchronous phenomenon and to allow the development of a suitable co-design condition. The term $x^\top Q_x x - e^\top Q_e e$ can be viewed as the deviation between the current state x_k and the last transmitted state \hat{x}_k , while $\pi^\top Q_\pi \pi - \delta^\top Q_\delta \delta$ can be viewed as the deviation between the current vector of nonlinearities π_k and the last transmitted vector of nonlinearities $\hat{\pi}_k$. Thus, the dynamic ETC scheme determines the appropriate transmission instants of the states in Fig. 1.

The next lemma establishes the positiveness of η according to (15). This property is required to construct a suitable Lyapunov function candidate to derive the co-design condition.

Lemma 1. Consider the dynamic ETC scheme (14)–(16) with initial condition $\eta_0 \geq 0$. If $\theta \geq 1/(1-\lambda)$, then $\eta_k \geq 0$, $\forall k \in \mathbb{N}_0$.

Proof. The proof follows from (Hu et al., 2016, Lemma 1). By construction, it is not difficult to see that (14) guarantees that $\eta_k + \theta\Gamma(\zeta) \geq 0, \forall k \in \mathbb{N}$. Note that when $\theta = 0$, $\eta_k \geq 0$. If $\theta \neq 0$, and using (15), then $\eta_{k+1} \geq$

$(1 - \frac{1}{\theta} - \lambda) \eta_k$. Using the last inequality iteratively and noting that $\eta_0 \geq 0$, it follows that $\eta_k \geq (1 - \frac{1}{\theta} - \lambda)^k \eta_0 \geq 0, \forall k \in \mathbb{N}$. Provided that $\eta_0 \geq 0$, then $\eta_k \geq 0 \forall k \in \mathbb{N}_0$, under $\theta \geq 1/(1 - \lambda)$. This completes the proof. ■

3.2 Co-design condition

The condition to co-design the control gains and the parameters of the dynamic ETM are presented in Theorem 1.

Theorem 1. Consider the discrete-time dynamical system in (1) represented in a DAR form as in (2), the control law (9), and the dynamic ETM described in (14)–(16). Let $\eta_0, \theta \in \mathbb{R}_{\geq 0}, \lambda \in \mathbb{R}_{>0}$, being given scalars satisfying $\theta > 1/(1 - \lambda)$. If there exist matrices $\tilde{L}_j \in \mathbb{R}^{m \times p}, \tilde{K}_j \in \mathbb{R}^{m \times n}, \mathbf{j} \in \mathbb{B}^r, \tilde{Z} \in \mathbb{R}^{p \times p}$, and symmetric positive definite matrices $\tilde{Q}_x, \tilde{Q}_e, X \in \mathbb{R}^{n \times n}$ and $\tilde{Q}_\pi, \tilde{Q}_\delta \in \mathbb{R}^{p \times p}$, such that the following LMIs hold:

$$\begin{bmatrix} 1 & b_j^\top X \\ * & X \end{bmatrix} \geq 0, \quad j \in \mathbb{N}_{\leq h}, \quad (18)$$

$$\sum_{(\mathbf{i}, \mathbf{j}) \in \mathcal{P}(\mathbf{m}, \mathbf{n})} \Phi_{\mathbf{ij}} < 0, \quad \forall \mathbf{m}, \mathbf{n} \in \mathbb{B}^{r+}, \quad (19)$$

with

$$\Phi_{\mathbf{ij}} = \begin{bmatrix} -X & 0 & \Phi_{1,3} & 0 & \Phi_{1,5} & X & 0 \\ * & -\tilde{Q}_e & \tilde{K}_j^\top \Omega_{3i}^\top & 0 & \tilde{K}_j^\top A_{3i}^\top & 0 & 0 \\ * & * & \Phi_{3,3} & \Omega_{3i} \tilde{L}_j^\top & \Phi_{3,5} & 0 & \tilde{Z}^\top \\ * & * & * & -\tilde{Q}_\delta & \tilde{L}_j^\top A_{3i}^\top & 0 & 0 \\ * & * & * & * & -X & 0 & 0 \\ * & * & * & * & * & -\tilde{Q}_x & 0 \\ * & * & * & * & * & * & -\tilde{Q}_\pi \end{bmatrix},$$

$$\Phi_{1,3} = X \Omega_{1i}^\top + \tilde{K}_j^\top \Omega_{3i}^\top, \quad \Phi_{1,5} = X A_{1i}^\top + \tilde{K}_j^\top A_{3i}^\top,$$

$$\Phi_{3,3} = \text{He}(\Omega_{2i} \tilde{Z} + \Omega_{3i} \tilde{L}_j), \quad \Phi_{3,5} = \tilde{Z}^\top A_{2i}^\top + \tilde{L}_j^\top A_{3i}^\top,$$

then, the origin of the closed-loop system (13) is asymptotically stable with the control gains given by $K_j = \tilde{K}_j X^{-1}, L_j = \tilde{L}_j \tilde{Z}^{-1}, \mathbf{j} \in \mathbb{B}^r$, and ETM parameters given by $Q_e = X^{-1} \tilde{Q}_e X^{-1}, Q_x = \tilde{Q}_x^{-1}, Q_\delta = \tilde{Z}^{-\top} \tilde{Q}_\delta \tilde{Z}^{-1}, Q_\pi = \tilde{Q}_\pi^{-1}, P = X^{-1}, Z = \tilde{Z}^{-\top}$. Moreover, the Lyapunov function that certifies the asymptotic stability of the origin is

$$W(x, \eta) = V(x) + \eta, \quad V(x) = x^\top P x, \quad (20)$$

and, for a given η_0 , the state trajectories (x_k, η_k) with initial condition x_0 taken inside of

$$\mathcal{R}_0 = \{x \in \mathbb{R}^n : V(x) \leq 1 - \eta_0, \eta_0 < 1\}, \quad (21)$$

converge asymptotically to the origin $(x, \eta) = (0, 0)$ without leaving the region

$$\mathcal{R} = \{x \in \mathbb{R}^n, \eta \in \mathbb{R}_{>0} : W(x, \eta) \leq 1\}, \quad (22)$$

which, in its turn, satisfies $\mathcal{R} \subset \mathcal{D}_x \times \mathbb{R}_{\geq 0}$.

Proof. Considering the Lyapunov function candidate (20), Lemma 1, and X is a symmetric positive definite matrix. Suppose that the inequalities in (19) hold. Then, it follows that

$$\Phi(x) = \sum_{\mathbf{m} \in \mathbb{B}} \sum_{\mathbf{n} \in \mathbb{B}} \alpha_{\mathbf{m}}(x) \alpha_{\mathbf{n}}(x) \left(\sum_{(\mathbf{i}, \mathbf{j}) \in \mathcal{P}(\mathbf{m}, \mathbf{n})} \Phi_{\mathbf{ij}} \right) < 0. \quad (23)$$

Multiplying (23) by $\text{diag}\{X^{-1}, X^{-1}, \tilde{Z}^{-1}, \tilde{Z}^{-1}, X^{-1}, I, I\}$ on the left and its transpose on the right, since $X > 0$ and \tilde{Z} is invertible, therefore

$$\Phi_{ij}^1 = \begin{bmatrix} -X^{-1} & 0 & \Phi_{1,3}^1 & 0 & \Phi_{1,5}^1 & I & 0 \\ * & \Phi_{2,2}^1 & \Phi_{2,3}^1 & 0 & \Phi_{2,5}^1 & 0 & 0 \\ * & * & \Phi_{3,3}^1 & \Phi_{3,4}^1 & \Phi_{3,5}^1 & 0 & I \\ * & * & * & \Phi_{4,4}^1 & \Phi_{4,5}^1 & 0 & 0 \\ * & * & * & * & -X^{-1} & 0 & 0 \\ * & * & * & * & * & -\tilde{Q}_x & 0 \\ * & * & * & * & * & * & -\tilde{Q}_\pi \end{bmatrix} < 0, \quad (24)$$

with

$$\begin{aligned} \Phi_{1,3}^1 &= (\Omega_{1i}^\top + X^{-1} \tilde{K}_j^\top \Omega_{3i}^\top) \tilde{Z}^{-1}, \\ \Phi_{1,5}^1 &= (A_{1i}^\top + X^{-1} \tilde{K}_j^\top A_{3i}^\top) X^{-1}, \quad \Phi_{2,2}^1 = -X^{-1} \tilde{Q}_e X^{-1}, \\ \Phi_{2,3}^1 &= X^{-1} \tilde{K}_j^\top \Omega_{3i}^\top \tilde{Z}^{-1}, \quad \Phi_{2,5}^1 = X^{-1} \tilde{K}_j^\top A_{3i}^\top X^{-1}, \\ \Phi_{3,3}^1 &= \text{He}(\tilde{Z}^{-\top} (\Omega_{2i} + \Omega_{3i} \tilde{L}_j \tilde{Z}^{-1})), \\ \Phi_{3,4}^1 &= \tilde{Z}^{-\top} \Omega_{3i} \tilde{L}_j \tilde{Z}^{-1}, \quad \Phi_{3,5}^1 = (A_{2i}^\top + \tilde{Z}^{-\top} \tilde{L}_j^\top A_{3i}^\top) X^{-1}, \\ \Phi_{4,4}^1 &= \tilde{Z}^{-\top} \tilde{Q}_\delta \tilde{Z}^{-1}, \quad \Phi_{4,5}^1 = \tilde{Z}^{-\top} \tilde{L}_j^\top A_{3i}^\top X^{-1}. \end{aligned}$$

Applying the Schur complement and the change of variables $P = X^{-1}$, $Z = \tilde{Z}^{-\top}$, $K = \tilde{K}_j X^{-1}$, $L_j = \tilde{L}_j \tilde{Z}^{-1}$, $Q_x = \tilde{Q}_x^{-1}$, $Q_e = X^{-1} \tilde{Q}_e X^{-1}$, $Q_\delta = \tilde{Z}^{-\top} \tilde{Q}_\delta \tilde{Z}^{-1}$, $Q_\pi = \tilde{Q}_\pi^{-1}$, $A_K = A_{1i} + A_{3i} K_j$, $\Omega_K = \Omega_{1i} + \Omega_{3i} K_j$, $A_L = A_{2i} + A_{3i} L_j$, $\Omega_L = \Omega_{2i} + \Omega_{3i} L_j$, it results in

$$\begin{bmatrix} \Psi_{11} & \Psi_{12} \\ * & \Psi_{22} \end{bmatrix} < 0, \quad (25)$$

where

$$\begin{aligned} \Psi_{11} &= \begin{bmatrix} A_K^\top P A_K - P + Q_x & A_K^\top P A_3 K \\ * & K^\top A_3^\top P A_3 K - Q_e \end{bmatrix}, \\ \Psi_{12} &= \begin{bmatrix} A_K^\top P A_L + \Omega_K^\top Z^\top & A_K^\top P A_3 L \\ K^\top A_3^\top P A_L + K^\top \Omega_3^\top Z^\top & K^\top A_3^\top P A_3 L \end{bmatrix}, \\ \Psi_{22} &= \begin{bmatrix} \text{He}(Z \Omega_L) + A_L^\top P A_L + Q_\pi & A_L^\top P A_3 L + Z \Omega_3 L \\ * & L^\top A_3^\top P A_3 L - Q_\delta \end{bmatrix}. \end{aligned}$$

Multiplying (25) by ζ^\top on the left and its transpose on the right, then adding the term $\xi(\zeta)$, given by (17), on both sides of the inequality, it follows that

$$\begin{aligned} (\varphi_1 + \xi_1)^\top P (\varphi_1 + \xi_1) - x^\top P x \\ + 2\pi^\top Z (\varphi_2 + \xi_2) + x^\top Q_x x + \pi^\top Q_\pi \pi \\ - e^\top Q_e e - \delta^\top Q_\delta \delta - \xi(\zeta) < 0. \end{aligned} \quad (26)$$

Using the DAR in (13), the trigger function (16), and Lemma 1, for some given $\eta_0, \theta \in \mathbb{R}_{\geq 0}$, $\lambda \in \mathbb{R}_{> 0}$, leads to

$$x_+^\top P x_+ - x^\top P x - \lambda \eta_k + \Gamma(\zeta) < 0, \quad (27)$$

or, equivalently,

$$\Delta W(x, \eta) := x_+^\top P x_+ - x^\top P x + \eta_{k+1} - \eta_k < 0. \quad (28)$$

The above inequality ensures $\Delta W(x, \eta) < 0$, $\forall (x, \eta) \neq (0, 0)$, and (20) is a Lyapunov function that certifies the asymptotic stability of the origin of the closed-loop system (13). It then follows from (28) that $W(x_k, \eta_k) \leq W(x_0, \eta_0) = V(x_0) + \eta_0$. Then, if $x_0 \in \mathcal{R}_0$, for some $\eta_0 \in [0, 1)$, it follows that $W(x_k, \eta_k) \leq 1$, which means that $(x_k, \eta_k) \in \mathcal{R}$, $\forall k \in \mathbb{N}_0$.

By applying a congruence transformation to (18) with the matrix $\text{diag}\{1, X^{-1}\}$, then multiplying the result by $[1 \ x^\top]$ on the right and its transpose on the left, it follows

that $1 - 2b_j^\top x + V(x) \geq 0$, $\forall j \in \mathbb{N}_{\leq 0}$. By summing and subtracting η , yields $1 - 2b_j^\top x + W(x, \eta) - \eta \geq 0$, $\forall j \in \mathbb{N}_{\leq 0}$. Then, if $(x, \eta) \in \mathcal{R}$, it follows that $2 - 2b_j^\top x - \eta \geq 0$, $\forall j \in \mathbb{N}_{\leq 0}$, which implies from the fact that $\eta_k \geq 0$, $\forall k \in \mathbb{N}_0$, that $b_j^\top x \leq 1$, $\forall j \in \mathbb{N}_{\leq 0}$, and $x \in \mathcal{D}_x$. This implies that $\mathcal{R} \subset \mathcal{D}_x \times \mathbb{R}_{\geq 0}$.

Thus, if $x_0 \in \mathcal{R}_0$ for some $\eta_0 \in [0, 1)$, then (x_k, η_k) converge asymptotically to the origin $(x, \eta) = (0, 0)$, without leaving the region $\mathcal{R} \subset \mathcal{D}_x \times \mathbb{R}_{\geq 0}$, which ensures that the closed-loop trajectories do not leave the domain of validity of the DAR, \mathcal{D}_x , given in (3). This concludes the proof. \blacksquare

Remark 2. An outstanding feature of the methodology proposed to establish Theorem 1 is the incorporation of the vector of nonlinearities of the DAR (2) into the gain-scheduled control law (9) and the trigger function (16). While in Reis et al. (2025), in addition to dealing the continuous-time case, a control law independent of the vector of nonlinearities is designed.

In the sequel, similarly to Reis et al. (2025), we derive another co-design condition to design the following gain-scheduled controller

$$u_k = K(\hat{x}_k) \hat{x}_k, \quad (29)$$

which is a particular case of (9) without the nonlinearity term, that is, $L(\hat{x}_k) = 0$, and the following trigger function:

$$\Gamma(x, e, \pi) = x^\top Q_x x - e^\top Q_e e - \xi(x, e, \pi), \quad (30)$$

where $\xi(x, e, \pi)$ is given as in (17) taking $L(\hat{x}) = 0$. The co-design condition is established in the following Corollary.

Corollary 1. Consider the discrete-time dynamical system in (1) represented in a DAR form as in (2), the control law (29), and the dynamic ETM described by (14), (15), (29). Under the conditions of Theorem 1, if (18) and the following LMIs hold:

$$\sum_{(i,j) \in \mathcal{P}(\mathbf{m}, \mathbf{n})} \Phi_{ij} < 0, \quad \forall \mathbf{m}, \mathbf{n} \in \mathbb{B}^{r+}, \quad (31)$$

with

$$\Phi_{ij} = \begin{bmatrix} -X & 0 & \Phi_{1,3} & \Phi_{1,4} & X \\ * & -\tilde{Q}_e & \tilde{K}_j^\top \Omega_{3i}^\top & \tilde{K}_j^\top A_{3i}^\top & 0 \\ * & * & \text{He}(\Omega_{2i} \tilde{Z}) & \tilde{Z}^\top A_{2i}^\top & 0 \\ * & * & * & -X & 0 \\ * & * & * & * & -\tilde{Q}_x \end{bmatrix},$$

$$\Phi_{1,3} = X \Omega_{1i}^\top + \tilde{K}_j^\top \Omega_{3i}^\top, \quad \Phi_{1,4} = X A_{1i}^\top + \tilde{K}_j^\top A_{3i}^\top.$$

then, the origin of the closed-loop system (13) with $L(x) = 0$ is asymptotically stable. Moreover, the Lyapunov function that certifies the asymptotic stability of the origin is given by (20) and, for a given η_0 , the state trajectories (x_k, η_k) with initial condition x_0 taken inside of (21) converge asymptotically to the origin $(x, \eta) = (0, 0)$ without leaving the region \mathcal{R} in (22), which, in its turn, satisfies $\mathcal{R} \subset \mathcal{D}_x \times \mathbb{R}_{\geq 0}$.

Proof. The proof follows the same steps as in Theorem 1. \blacksquare

3.3 Optimization problems

Sufficient co-design conditions for the event-based stabilization of the closed-loop system (13) were established

in the previous section. This section presents methods to increase the inter-transmission intervals and enlarge the region of attraction estimation of the origin of the closed-loop system.

To accomplish the objective of increasing the inter-transmission intervals, we follow a similar approach as in Coutinho et al. (2022); Moreira et al. (2020). According to the dynamic ETC scheme (14)–(16), a new transmission occurs when

$$\mathcal{G}(\zeta_k) > 1 + \frac{\eta_k}{\theta \mathcal{D}(x_k, \pi_k)} - \mathcal{V}(\zeta_k), \quad (32)$$

where

$$\mathcal{G}(\zeta) = \frac{e^\top Q_e e + \delta^\top Q_\delta \delta}{\mathcal{D}(x, \pi)}, \quad (33)$$

$$\mathcal{V}(\zeta) = \frac{\xi(\zeta)}{\mathcal{D}(x, \pi)}, \quad (34)$$

$$\mathcal{D}(x, \pi) = x^\top Q_x x + \pi^\top Q_\pi \pi. \quad (35)$$

Note that $\mathcal{G}(\zeta_k) = \mathcal{V}(\zeta_k) = 0$ at the transmission instants $k = k_j$. Alternatively, transmissions are not triggered while

$$\mathcal{G}(\zeta_k) \leq \frac{\lambda_{\max}(Q_e) \|e_k\|^2 + \lambda_{\max}(Q_\delta) \|\delta_k\|^2}{\lambda_{\min}(Q_x) \|x_k\|^2 + \lambda_{\min}(Q_\pi) \|\pi_k\|^2}, \quad (36)$$

that can be recast in the form

$$\mathcal{G}(\zeta_k) \leq \Lambda \frac{\|e_k\|^2 + \|\delta_k\|^2}{\|x_k\|^2 + \|\pi_k\|^2}, \quad (37)$$

where

$$\Lambda = \frac{\max\{\lambda_{\max}(Q_e), \lambda_{\max}(Q_\delta)\}}{\min\{\lambda_{\min}(Q_x), \lambda_{\min}(Q_\pi)\}}. \quad (38)$$

As a result, additional transmissions are not triggered unless

$$\frac{\|e_k\|^2 + \|\pi_k\|^2}{\|x_k\|^2 + \|\delta_k\|^2} \leq \frac{1}{\Lambda} \left(1 + \frac{\eta_k}{\theta \mathcal{D}(x_k, \pi_k)} - \mathcal{V}(\zeta_k) \right). \quad (39)$$

Then, minimizing Λ tends to increase the minimum time for $\mathcal{G}(x, e)$ to evolve from 0 to $1 + \eta/(\theta \mathcal{D}(x, \pi)) - \mathcal{V}(\zeta)$. This objective can be achieved by maximizing $\min\{\lambda_{\min}(Q_x), \lambda_{\min}(Q_\pi)\}$ and minimizing $\max\{\lambda_{\max}(Q_e), \lambda_{\max}(Q_\delta)\}$.

To achieve the second objective, recall that the set of admissible initial states is given by \mathcal{R}_0 in (21). If the conditions in Theorem 1 are fulfilled, for $x_0 \in \mathcal{R}_0$, we ensure that the trajectories of the closed-loop system (13) asymptotically converge to the origin without leaving the region $\mathcal{R} \subset \mathcal{D}_x \times \mathbb{R}_{\geq 0}$ in (22). This ensures that the closed-loop system operates inside the region of validity of the DAR model (2). Thus, the region of attraction estimation \mathcal{R} can be maximized by enlarging the region \mathcal{R}_0 , which can be viewed as a projection of \mathcal{R} onto $\mathcal{D}_x \subset \mathbb{R}^n$.

To simultaneously deal with these two objectives, we consider the ϵ -constraint optimization algorithm, resulting in the objective problem (OP) stated below, that is solved for a given value of $\epsilon > 0$.

$$\min_{\tilde{Q}_x, \tilde{Q}_e, \tilde{Q}_\pi, \tilde{Q}_\delta, X, \tilde{K}_j, \tilde{L}_j} \sigma \quad (40)$$

$$\text{subject to } \text{tr}(\tilde{Q}_x + \tilde{Q}_e) + \text{tr}(\tilde{Q}_\pi + \tilde{Q}_\delta) < \epsilon, \quad (41)$$

$$\begin{bmatrix} \sigma I & I \\ * & X \end{bmatrix} \geq 0, \quad (42)$$

LMI in (18), (19).

Applying Schur complement and change the variable $P = X^{-1}$ to the constraint (42), it follows that $P < \sigma I$. Thus, minimizing σ increase the region \mathcal{R}_0 since $V(x) \leq \sigma x^\top x$.

We state below the optimization problem as a consequence of Corollary 1 corresponding to the case where the control law (29) and the trigger function (30) without the nonlinearity dependence are employed.

$$\min_{\tilde{Q}_x, \tilde{Q}_e, X, \tilde{K}_j} \sigma \quad (43)$$

$$\text{subject to } \text{tr}(\tilde{Q}_x + \tilde{Q}_e) < \epsilon,$$

LMI in (18), (31), (42).

By solving the OP 1 in (40) and the OP 2 in (43) for different values of ϵ , we can obtain different values of σ . Thus, the pairs (ϵ, σ) obtained from the solutions of those OPs constitute an estimate of the Pareto front.

4. NUMERICAL RESULTS

In this section, an example is presented to show the effectiveness of the proposed dynamic ETC scheme of discrete-time nonlinear systems in the DAR form. Consider the following discretized nonlinear system:

$$\begin{aligned} x_{(1)k+1} &= x_{(1)k} + T x_{(2)k} \\ x_{(2)k+1} &= x_{(2)k} + T x_{(1)k} + T x_{(1)k}^3 \\ &\quad + 2T x_{(2)k} + 8T x_{(2)k}^3 + T u_k, \end{aligned} \quad (44)$$

where $T = 0.1$ s is the sampling period.

The system (44) can be described in the form of a DAR as (2) with

$$\begin{aligned} A_1 &= \begin{bmatrix} 1 & T \\ T & 1 + 2T \end{bmatrix}, A_2(x) = \begin{bmatrix} 0 & 0 \\ T x_{(1)} & 8T x_{(2)} \end{bmatrix}, A_3 = \begin{bmatrix} 0 \\ T \end{bmatrix}, \\ \Omega_1(x) &= \begin{bmatrix} x_{(1)} & 0 \\ 0 & x_{(2)} \end{bmatrix}, \Omega_2 = \begin{bmatrix} -1 & 0 \\ 0 & -1 \end{bmatrix}, \Omega_3 = \begin{bmatrix} 0 \\ 0 \end{bmatrix}, \end{aligned} \quad (45)$$

and the vector of nonlinearities $\pi = [x_{(1)}^2 \ x_{(2)}^2]^\top$. It is assumed that the system trajectories are constrained by $\mathcal{D}_x = \{x \in \mathbb{R}^2 : |x_{(i)}| \leq \bar{x}, i = 1, 2\}$.

The solutions in Fig. 2, represented by the blue dashed line, were obtained by solving the optimization problem in OP 1 in (40) with $\bar{x} = 2$ for a set of 20 values of ϵ spaced on a logarithmic scale between 10^{-1} and 10^5 . For the considered region \mathcal{D}_x with $\bar{x} = 2$, no feasible solutions were obtained from the optimization problem in OP 2 in (43). The results show a trade-off between the two objectives, because a larger region of attraction requires a smaller σ , which forces the system to trigger more events. Then, by exploiting the solutions in the estimated Pareto front, a designer can choose to expand the estimated region of attraction or reduce the number of transmissions.

To evaluate the conservativeness of OP 2 in (43), we searched for the maximum value of \bar{x} for which OP 2 was

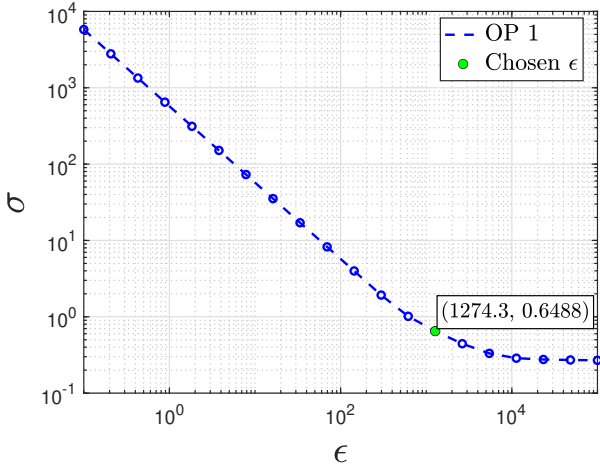


Fig. 2. The Pareto optimal solutions found via OP 1 in (40) in blue. The green marker indicates the point on the Pareto front corresponding to the chosen value of ϵ .

feasible. The maximum value of \bar{x} region of validity found in which OP 2 in (43) is feasible was $\bar{x} = 1.53$, leading to $\tilde{\mathcal{D}}_x = \{x \in \mathbb{R}^2 : |x_{(i)}| \leq 1.53, i = 1, 2\}$. In Fig. 3, we show the largest estimated regions of attraction obtained considering $\tilde{\mathcal{D}}_x$ to OP 1 in (40) and OP 2 in (43) solved with $\epsilon = 10^3$. This clearly indicates that the inclusion of the nonlinear term π in the control law reduces the conservativeness in the proposed approach, as a larger region of attraction estimate was obtained with $\bar{x} = 1.53$, and only OP 1 resulted in feasible solutions with $\bar{x} = 2$.

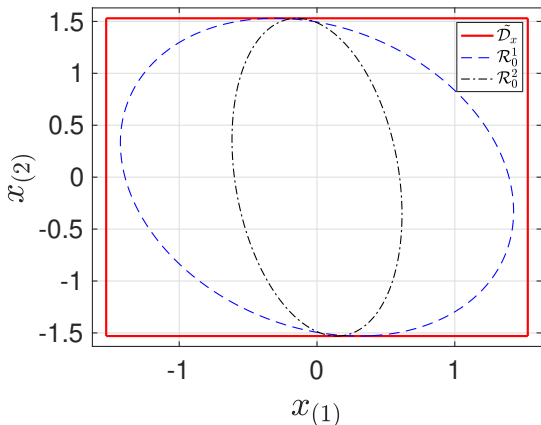


Fig. 3. Estimated regions of attraction. Validity region $\tilde{\mathcal{D}}_x$ is depicted as a red solid square. The blue dashed ellipse \mathcal{R}_0^1 corresponds to the estimated region for OP 1 in (40) while the black dash-dotted ellipse \mathcal{R}_0^2 corresponds to the estimated region for OP 2 in (43).

The estimation of the region of attraction obtained with $\epsilon = 1274.3$, considering the region \mathcal{D}_x is shown in Fig. 4 together with several closed-loop trajectories with initial conditions x_0 taken at the border of the region of admissible initial conditions \mathcal{R}_0 and $\eta_0 = 0$. Notice that all trajectories asymptotically converge to the origin $x = 0$.

We also compare the static and dynamic ETC schemes using the same selected $\epsilon = 1274.3$ and $\bar{x} = 2$, for which

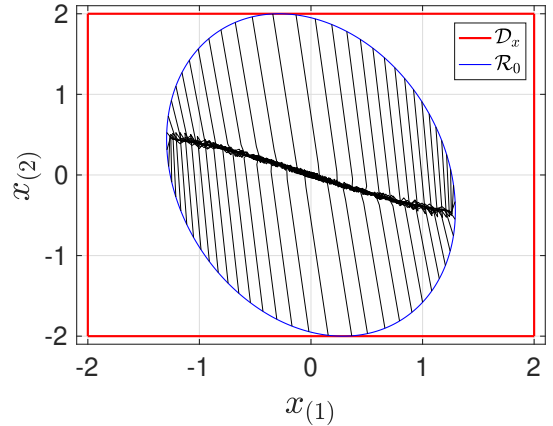


Fig. 4. The validity region \mathcal{D}_x and the estimated region of attraction \mathcal{R}_0 for OP 1 in (40).

only OP 1 is feasible. Table 1 summarizes the average number of events for both the static and dynamic ETC schemes designed via OP 1 in (40). The dynamic ETC scheme was evaluated with different values of λ and θ . We simulated the closed-loop system with 60 different initial conditions within the estimated region of attraction. It can be observed that the proposed dynamic ETC scheme effectively reduces the number of events.

Table 1. Average number of events considering 10 seconds interval.

Static ETC	34.79		
Dynamic ETC	$\lambda = 10^{-3}$	$\lambda = 10^{-2}$	$\lambda = 10^{-1}$
$\theta = 2$	34.31	34.38	34.51
$\theta = 10$	32.25	32.31	34.67
$\theta = 10^2$	32.10	32.41	34.78
$\theta = 10^3$	32.75	33.03	34.63

The time-series of a state trajectory of the closed-loop system, the sampled control input signal, and the inter-event transmission times are depicted in Fig. 5 for an initial condition set $x_0 = (0.6573, 1.4554)$, and parameter $\lambda = 10^{-3}$ and $\theta = 100$. In this simulation, 30 events were transmitted with the dynamic ETC scheme. Using the static version, 35 events are transmitted, and a standard periodic time-triggered scheme transmits 101 events. This illustrates that the proposed dynamic ETC scheme can save communication resources compared to its static counterpart and a standard periodic time-triggered scheduler.

5. CONCLUSION

In this paper, a dynamic ETC scheme for discrete-time nonlinear systems based on DAR was addressed. The proposed co-design condition ensured the asymptotic stability of the origin of the closed-loop system. The co-design of the ETC scheme with a nonlinear gain-scheduled controller was established through a Lyapunov-based analysis. Furthermore, an optimization problem was employed to reduce the number of transmissions and enlarge the region of attraction estimation. The numerical example validated the proposed methodology, revealing that the nonlinear gain-scheduled controller provided a less conservative condition than both a standard gain-scheduled controller and

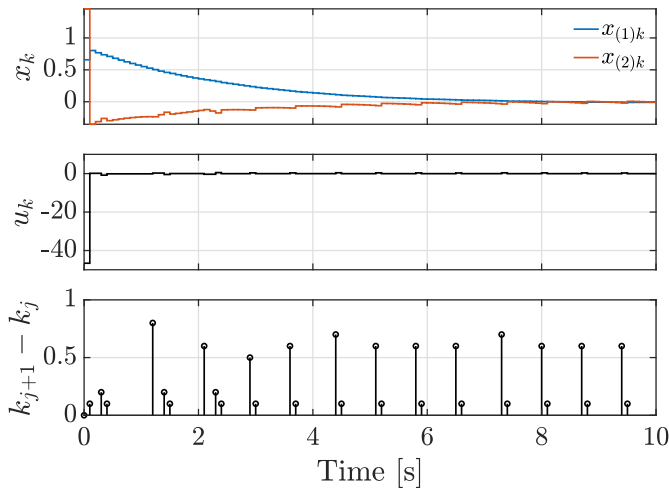


Fig. 5. Trajectory of states in a closed-loop with dynamic ETM.

a linear one. Finally, as expected, the dynamic ETC scheme outperformed the static approach by reducing the occurrence of triggering events.

REFERENCES

- Abdelrahim, M., Postoyan, R., Daafouz, J., Nešić, D., and Heemels, M. (2018). Co-design of output feedback laws and event-triggering conditions for the \mathcal{L}_2 -stabilization of linear systems. *Automatica*, 87, 337–344.
- Azizi, S., Torres, L.A.B., and Palhares, R.M. (2018). Regional robust stabilisation and domain-of-attraction estimation for mimo uncertain nonlinear systems with input saturation. *International Journal of Control*, 91(1), 215–229.
- Coutinho, D.F., de Souza, C.E., and Barbosa, K.A. (2009). Robust \mathcal{H}_∞ filter design for a class of discrete-time parameter varying systems. *Automatica*, 45(12), 2946–2954.
- Coutinho, D.F. and Gomes da Silva Jr., J.M. (2010). Computing estimates of the region of attraction for rational control systems with saturating actuators. *IET Control Theory & Applications*, 4, 315–325.
- Coutinho, P.H.S., Bessa, I., and Palhares, R.M. (2025). Resilient dynamic event-triggered fuzzy control against DoS attacks on cyber-physical systems. *Journal of Control, Automation and Electrical Systems*, 36, 402–412.
- Coutinho, P.H.S. and Palhares, R.M. (2021). Dynamic periodic event-triggered gain-scheduling control co-design for quasi-LPV systems. *Nonlinear Analysis: Hybrid Systems*, 41, 101044.
- Coutinho, P.H.S. and Palhares, R.M. (2022). Codesign of dynamic event-triggered gain-scheduling control for a class of nonlinear systems. *IEEE Transactions on Automatic Control*, 67(8), 4186–4193.
- Coutinho, P.H.S., Peixoto, M.L.C., Bessa, I., and Palhares, R.M. (2022). Dynamic event-triggered gain-scheduling control of discrete-time quasi-LPV systems. *Automatica*, 141, 110292.
- Girard, A. (2015). Dynamic triggering mechanisms for event-triggered control. *IEEE Transactions on Automatic Control*, 60(7), 1992–1997.
- Hu, S., Yue, S., Yin, X., Xie, X., and Ma, Y. (2016). Adaptive event-triggered control for nonlinear discrete-time systems. *International Journal of Robust and Nonlinear Control*, 26(18), 4104–4125.
- Li, Z., Yan, J., Yu, W., and Qiu, J. (2021). Adaptive event-triggered control for unknown second-order nonlinear multiagent systems. *IEEE Transactions on Cybernetics*, 51(12), 6131–6140.
- Moreira, L.G., Gomes da Silva Jr., J.M., Coutinho, D.F., and Tarbouriech, S. (2020). Event-triggered control co-design for rational systems. *IFAC-PapersOnLine*, 53(2), 2720–2725. 21st IFAC World Congress.
- Moreira, L.G., Groff, L.B., Gomes da Silva Jr., J.M., and Coutinho, D.F. (2017). Event-triggered control for nonlinear rational systems. *IFAC-PapersOnLine*, 50(1), 15307–15312. 20th IFAC World Congress.
- Oliveira, M.Z., Gomes da Silva Jr., J.M., and Coutinho, D. (2013a). Regional stabilization of rational discrete-time systems with magnitude control constraints. In *2013 American Control Conference*, 241–246.
- Oliveira, M.Z., Gomes da Silva Jr., J.M., and Coutinho, D.F. (2012). State feedback design for rational nonlinear control systems with saturating inputs. In *2012 American Control Conference (ACC)*, 2331–2336.
- Oliveira, M.Z., Gomes da Silva Jr., J.M., and Coutinho, D.F. (2013b). Stability analysis for a class of nonlinear discrete-time control systems subject to disturbances and to actuator saturation. *International Journal of Control*, 86(5), 869–882.
- Pessim, P.S.P., Coutinho, P.H.S., Lacerda, M.J., and Palhares, R.M. (2023). Distributed event-triggered fuzzy control for nonlinear interconnected systems. *Chaos, Solitons & Fractals*, 177, 114276.
- Reis, G.L., Araújo, R.F., Torres, L.A.B., and Palhares, R.M. (2021). Gain-scheduled control design for discrete-time nonlinear systems using difference-algebraic representations. *International Journal of Robust and Nonlinear Control*, 31(5), 1542–1563.
- Reis, G.L., Coutinho, P.H.S., Bessa, I., and Araújo, R.F. (2025). Dynamic event-triggered control for nonlinear systems via differential algebraic representation. *Nonlinear Analysis: Hybrid Systems*, 57, 101597.
- Rohr, E.R., Pereira, L.F.A., and Coutinho, D.F. (2009). Robustness analysis of nonlinear systems subject to state feedback linearization. *Sba: Controle & Automação Sociedade Brasileira de Automatica*, 20(4), 482–489.
- Xiao, F., Shi, Y., and Chen, T. (2021). Robust stability of networked linear control systems with asynchronous continuous- and discrete-time event-triggering schemes. *IEEE Transactions on Automatic Control*, 66(2), 932–939.
- Xu, C., Qin, Y., and Su, H. (2023). Observer-based dynamic event-triggered bipartite consensus of discrete-time multi-agent systems. *IEEE Transactions on Circuits and Systems II: Express Briefs*, 70(3), 1054–1058.
- Zuo, Z., Cheng, H., Wang, Y., and Li, H. (2019). Event-triggered composite nonlinear control for saturated systems with measurement feedback. *Transactions of the Institute of Measurement and Control*, 41(14), 3943–3951.